Application of an improved high order PDE in image edge detection

Yu Bowen

***Abstract*—The two order partial differential equation in the image edge detection, has good edge holding ability, but there will be a "piecewise constant" effect, leading to false edges produced. Partial differential equation of higher order is very good to overcome the "piecewise constant" effect, but the ability of keeping edge drop, resulting in blurred edge. Therefore, this paper proposes a model for edge detection fusion of two order partial differential equation with four order partial differential equations, gives the Euler Lagrange equation and the gradient descent flow, and introduces the numerical discretization method.Finally a numerical validation is performed by the edge detection of objective evaluation index. Experiments show that, this method is very effectively in the image edge extraction, and overcome "piecewise constant" effect , edge blur and other shortcomings, improving the extraction results.**

***Index Terms*—the two order PDE, four order PDE, edge detection, evaluation index**

I. INTRODUCTION

Image edge detection, which is a key technology in the machine vision field [1], can make necessary early-stage preparation for later image processing such as image segmentation [2], image inpainting [3], and pattern recognition [4]. The traditional second-order partial differential equation models include the models based on heat diffusion equation (such as heat equation diffusion model [5], P-M diffusion model [6] and Catte diffusion model [7]) and the second-order models based on total variation (such as the classical TV model [8], General TV model [9] and self-adaption model [10]). The second-order partial differential equation model is able to preserve the edges well during the edge extraction process. However, it will generate a "piecewise constant effect" during the image smoothing process, result in the existence of false edge and, thus, affect the extraction effect. The four-order differential equation models arisen in recent years include the Y-K model [11] and the improved Y-K model [12]. They can successfully overcome the shortcomings caused by second-order partial differential models but will cause the shortcomings such as "speckle effect" [13] edge blur [14] in images and inaccurate edge extraction and positioning during the smoothing process.

After the analysis on the advantages and disadvantages of the traditional second-order and four-order partial differential equations during the edge extraction process, an improved high-order partial differential model was obtained through the integration between the second-order and four-order models. Its gradient descent flow was given through the Euler-Langrange equation. Finally, the experimental verification was conducted through the numerical discretization method and in combination with the objective evaluation indexes of edge detection. The result shows that the model is improved to some degree when it is compared with the traditional second-order and four-order partial differential models based on the objective evaluation indexes of edge detection.

YU Bo-wen, Automatization Engineering College, Nanjing University of Science and Technology, Nanjing, China, 18545055186.

II. NEW MODEL OF IMPROVED HIGH-ORDER PARTIAL DIFFERENTIAL EQUATION

In a traditional second-order model, $|\nabla u|$ is used to describe the image smoothness; in a traditional high-order model, the Laplace operator $|\Delta u|$ is used to describe the image smoothness. In this paper, the new model integrating the second-order partial differential equation and the four-order partial differential equation is used namely,

$$\sqrt{(|u_x|+|u_{xx}|)^2+(|u_y|+|u_{yy}|)^2} \tag{1}$$

The operator is used to describe the image smoothness. Then, the energy functional obtained by the new model in the condition of noise variance constraint is:

$$E(u)=\iint_\Omega \sqrt{(|u_x|+|u_{xx}|)^2+(|u_y|+|u_{yy}|)^2}+\frac{\lambda}{2}(u-u_0)^2\,dxdy \tag{2}$$

In the formula above, the second item, which is a fidelity term, is used to approach the similarity between the processed image and the original one. λ is the regulation coefficient. Solving the Euler-Lagrange equation of the energy functional is to solve the minimum value of the functional. Change formula (2) into:

$$E(u)=\iint_\Omega \sqrt{\left(\sqrt{(u_x)^2}+\sqrt{(u_{xx})^2}\right)^2+\left(\sqrt{(u_y)^2}+\sqrt{(u_{yy})^2}\right)^2}+\frac{\lambda}{2}(u-u_0)^2\,dxdy \tag{3}$$

In the formula above, the integrand is:

$$F:\sqrt{\left(\sqrt{(u_x)^2}+\sqrt{(u_{xx})^2}\right)^2+\left(\sqrt{(u_y)^2}+\sqrt{(u_{yy})^2}\right)^2}+\frac{\lambda}{2}(u-u_0)^2 \tag{4}$$

Then, the first-order partial derivative and the second-order partial derivative in formula (4) is:

$$F_u=\lambda(u-u_0)$$

$$F_{u_x}=\frac{\left(\sqrt{(u_x)^2}+\sqrt{(u_{xx})^2}\right)\bullet\frac{u_x}{\sqrt{(u_x)^2}}}{\sqrt{\left(\sqrt{(u_x)^2}+\sqrt{(u_{xx})^2}\right)^2+\left(\sqrt{(u_y)^2}+\sqrt{(u_{yy})^2}\right)^2}}$$

$$F_{u_y}=\frac{\left(\sqrt{(u_y)^2}+\sqrt{(u_{yy})^2}\right)\bullet\frac{u_y}{\sqrt{(u_y)^2}}}{\sqrt{\left(\sqrt{(u_x)^2}+\sqrt{(u_{xx})^2}\right)^2+\left(\sqrt{(u_y)^2}+\sqrt{(u_{yy})^2}\right)^2}}$$

$$F_{u_{xx}}=\frac{\left(\sqrt{(u_x)^2}+\sqrt{(u_{xx})^2}\right)\bullet\frac{u_{xx}}{\sqrt{(u_{xx})^2}}}{\sqrt{\left(\sqrt{(u_x)^2}+\sqrt{(u_{xx})^2}\right)^2+\left(\sqrt{(u_y)^2}+\sqrt{(u_{yy})^2}\right)^2}}$$

$$F_{u_{yy}}=\frac{\left(\sqrt{(u_y)^2}+\sqrt{(u_{yy})^2}\right)\bullet\frac{u_{yy}}{\sqrt{(u_{yy})^2}}}{\sqrt{\left(\sqrt{(u_x)^2}+\sqrt{(u_{xx})^2}\right)^2+\left(\sqrt{(u_y)^2}+\sqrt{(u_{yy})^2}\right)^2}} \quad (5)$$

The Euler-Lagrange equation in formula (3) is:

$$F_u-\frac{\partial F_{u_x}}{\partial x}-\frac{\partial F_{u_y}}{\partial y}+\frac{\partial^2 F_{u_{xx}}}{\partial x^2}+\frac{\partial^2 F_{u_{yy}}}{\partial y^2}=0 \quad (6)$$

Put formula (5) into formula (6),then:

$$\lambda(u-u_0)-\left(\frac{\left(\sqrt{(u_x)^2}+\sqrt{(u_{xx})^2}\right)\bullet\frac{u_x}{\sqrt{(u_x)^2}}}{\sqrt{\left(\sqrt{(u_x)^2}+\sqrt{(u_{xx})^2}\right)^2+\left(\sqrt{(u_y)^2}+\sqrt{(u_{yy})^2}\right)^2}}\right)_x-\left(\frac{\left(\sqrt{(u_y)^2}+\sqrt{(u_{yy})^2}\right)\bullet\frac{u_y}{\sqrt{(u_y)^2}}}{\sqrt{\left(\sqrt{(u_x)^2}+\sqrt{(u_{xx})^2}\right)^2+\left(\sqrt{(u_y)^2}+\sqrt{(u_{yy})^2}\right)^2}}\right)_y+\left(\frac{\left(\sqrt{(u_x)^2}+\sqrt{(u_{xx})^2}\right)\bullet\frac{u_{xx}}{\sqrt{(u_{xx})^2}}}{\sqrt{\left(\sqrt{(u_x)^2}+\sqrt{(u_{xx})^2}\right)^2+\left(\sqrt{(u_y)^2}+\sqrt{(u_{yy})^2}\right)^2}}\right)_{xx}+\left(\frac{\left(\sqrt{(u_y)^2}+\sqrt{(u_{yy})^2}\right)\bullet\frac{u_{yy}}{\sqrt{(u_{yy})^2}}}{\sqrt{\left(\sqrt{(u_x)^2}+\sqrt{(u_{xx})^2}\right)^2+\left(\sqrt{(u_y)^2}+\sqrt{(u_{yy})^2}\right)^2}}\right)_{yy}=0 \quad (7)$$

Let

$$D=\sqrt{\left(\sqrt{(u_x)^2}+\sqrt{(u_{xx})^2}\right)^2+\left(\sqrt{(u_y)^2}+\sqrt{(u_{yy})^2}\right)^2} \quad (8)$$

Then, formula (7) can be simplified into:

$$\lambda(u-u_0)-\left(\frac{\left(\sqrt{(u_x)^2}+\sqrt{(u_{xx})^2}\right)\bullet\frac{u_x}{\sqrt{(u_x)^2}}}{D}\right)_x-\left(\frac{\left(\sqrt{(u_y)^2}+\sqrt{(u_{yy})^2}\right)\bullet\frac{u_y}{\sqrt{(u_y)^2}}}{D}\right)_y+\left(\frac{\left(\sqrt{(u_x)^2}+\sqrt{(u_{xx})^2}\right)\bullet\frac{u_{xx}}{\sqrt{(u_{xx})^2}}}{D}\right)_{xx}+\left(\frac{\left(\sqrt{(u_y)^2}+\sqrt{(u_{yy})^2}\right)\bullet\frac{u_{yy}}{\sqrt{(u_{yy})^2}}}{D}\right)_{yy}=0 \quad (9)$$

Continue to simplify formula (9):

$$\lambda(u-u_0)-\left(\frac{\left(|u_x|+|u_{xx}|\right)\bullet\frac{u_x}{|u_x|}}{D}\right)_x-\left(\frac{\left(|u_y|+|u_{yy}|\right)\bullet\frac{u_y}{|u_y|}}{D}\right)_y+\left(\frac{\left(|u_x|+|u_{xx}|\right)\bullet\frac{u_{xx}}{|u_{xx}|}}{D}\right)_{xx}+\left(\frac{\left(|u_y|+|u_{yy}|\right)\bullet\frac{u_{yy}}{|u_{yy}|}}{D}\right)_{yy}=0 \quad (10)$$

Therefore, the gradient descent flow of formula (10) is:

$$\frac{\partial u}{\partial t}=\left(\frac{\left(|u_x|+|u_{xx}|\right)\bullet\frac{u_x}{|u_x|}}{D}\right)_x+\left(\frac{\left(|u_y|+|u_{yy}|\right)\bullet\frac{u_y}{|u_y|}}{D}\right)_y-\left(\frac{\left(|u_x|+|u_{xx}|\right)\bullet\frac{u_{xx}}{|u_{xx}|}}{D}\right)_{xx}-\left(\frac{\left(|u_y|+|u_{yy}|\right)\bullet\frac{u_{yy}}{|u_{yy}|}}{D}\right)_{yy}-\lambda(u-u_0) \quad (11)$$

In order to weaken the influence of noise, Gaussian filter can be conducted before calculation of D, namely,

$$D_\sigma=\sqrt{\left|(G_\sigma*u)_x\right|+\left|(G_\sigma*u)_{xx}\right|^2+\left|\left|(G_\sigma*u)_y\right|+\left|(G_\sigma*u)_{yy}\right|\right|^2} \quad (12)$$

Then, formula (11) is changed into:

$$\frac{\partial u}{\partial t}=\left(\frac{\left(|u_x|+|u_{xx}|\right)\bullet\frac{u_x}{|u_x|}}{D_\sigma}\right)_x+\left(\frac{\left(|u_y|+|u_{yy}|\right)\bullet\frac{u_y}{|u_y|}}{D_\sigma}\right)_y-\left(\frac{\left(|u_x|+|u_{xx}|\right)\bullet\frac{u_{xx}}{|u_{xx}|}}{D_\sigma}\right)_{xx}-\left(\frac{\left(|u_y|+|u_{yy}|\right)\bullet\frac{u_{yy}}{|u_{yy}|}}{D_\sigma}\right)_{yy}-\lambda(u-u_0) \quad (13)$$

The numerical solution of image smoothing can be obtained through numerical discretization of formula (13).

III. NUMERICAL DISCRETIZATION METHOD

In this paper, the following difference scheme is used to discretize formula (13).

$$u_x=\frac{u_{i,j+1}-u_{i,j-1}}{2}$$
$$u_y=\frac{u_{i+1,j}-u_{i-1,j}}{2} \quad (14)$$

$$u_{xx}=u_{i,j+1}+u_{i,j-1}-2\times u_{i,j}$$
$$u_{yy}=u_{i+1,j}+u_{i-1,j}-2\times u_{i,j} \quad (15)$$

The corresponding first-order and second-order partial derivatives can be solved inside each bracket of formula (13) but the solving process must be very complicated. For the convenience of operation, we can directly use the first-order difference formula and second-order difference formula in formula (14) and formula (15) to solve the first-order and second-order partial derivatives outside the brace of formula (13).

Let

$$Z_1=\left(\frac{\left(|u_x|+|u_{xx}|\right)\bullet\frac{u_x}{|u_x|}}{D_\sigma}\right)\quad Z_2=\left(\frac{\left(|u_y|+|u_{yy}|\right)\bullet\frac{u_y}{|u_y|}}{D_\sigma}\right)$$
$$Z_3=\left(\frac{\left(|u_x|+|u_{xx}|\right)\bullet\frac{u_{xx}}{|u_{xx}|}}{D_\sigma}\right)\quad Z_4=\left(\frac{\left(|u_y|+|u_{yy}|\right)\bullet\frac{u_{yy}}{|u_{yy}|}}{D_\sigma}\right) \quad (16)$$

Then,

$$Z_1(i,j)_x = \frac{Z_1(i,j+1) - Z_1(i,j-1)}{2};$$
$$Z_2(i,j)_y = \frac{Z_2(i+1,j) - Z_2(i-1,j)}{2};$$
$$Z_3(i,j)_{xx} = Z_3(i,j+1) + Z_3(i,j-1) - 2\times Z_3(i,j)$$
$$Z_4(i,j)_{yy} = Z_4(i+1,j) + Z_4(i-1,j) - 2\times Z_4(i,j) \quad (17)$$

In order to prevent D_σ in formula (16) from equaling to 0 to result in the failure of calculation, add a tiny amended constant ε, which is greater than 0 in D; then, D_σ can be converted into $D_{\sigma\varepsilon}$, namely

$$D_{\sigma\varepsilon} = \sqrt{\varepsilon + \left|(G_\sigma * u)_x\right| + \left|(G_\sigma * u)_{xx}\right|^2 + \left|(G_\sigma * u)_y\right| + \left|(G_\sigma * u)_{yy}\right|^2} \quad (18)$$

As the high-order partial derivative existing in the formula, which is used to describe the image smoothing, will certainly bring in the interference of "speckle effect", we provide a discretization method [15] to get rid of the "speckle effect"; namely, calculate the four-directional mean m and variance σ^2 of pixel point $u_{i,j}$, and update the pixel value of $u_{i,j}$.

$$m = \frac{u_{i,j-1} + u_{i,j+1} + u_{i-1,j} + u_{i+1,j}}{4}$$
$$\sigma^2 = \frac{u_{i,j-1}^2 + u_{i,j+1}^2 + u_{i-1,j}^2 + u_{i+1,j}^2}{4} - m^2 \quad (19)$$

Only when $\left|u_{i,j} - m\right|^2 > \sigma^2$, let the pixel value $u_{i,j}$ be m; otherwise, it will stay the same.

IV. Detection Result and Data Analysis

Test the teaching Lena test image with the 512×512 international standard and the teaching building test image for crosswise comparison; then, compare the evaluation index of edge detection image obtained with the evaluation indexes of edge detection images respectively obtained from (1) heat equation diffusion model, (2) P-M diffusion model, (3) Catté diffusion model, (4) classical TV model, (5) General TV model and (6) self-adaption TV model among the traditional second-order models and the (1) classical Y-K model and (2) Y-K model improved based on the diffusion coefficient among the traditional four-order models.

As for the hardware testing environment, computers with the Core i5 processor (2.4GHz) and 4GB of physical memory in the laboratory are chosen uniformly; as for the software testing environment, the Matlab2012b version is chosen uniformly. Let the number of procedure iterations be 200 times, the time step be 0.01, the regularization parameter be 0.01 and the gradient threshold be 15.

A. *Experiment I*

We used Lena as the test image. Namely, we used the original pollution-free Lena test image to verify the validity of the new model in the condition of not adding Gaussian white noise. The test results for the 9 types of models are shown in Fig. 1 below:

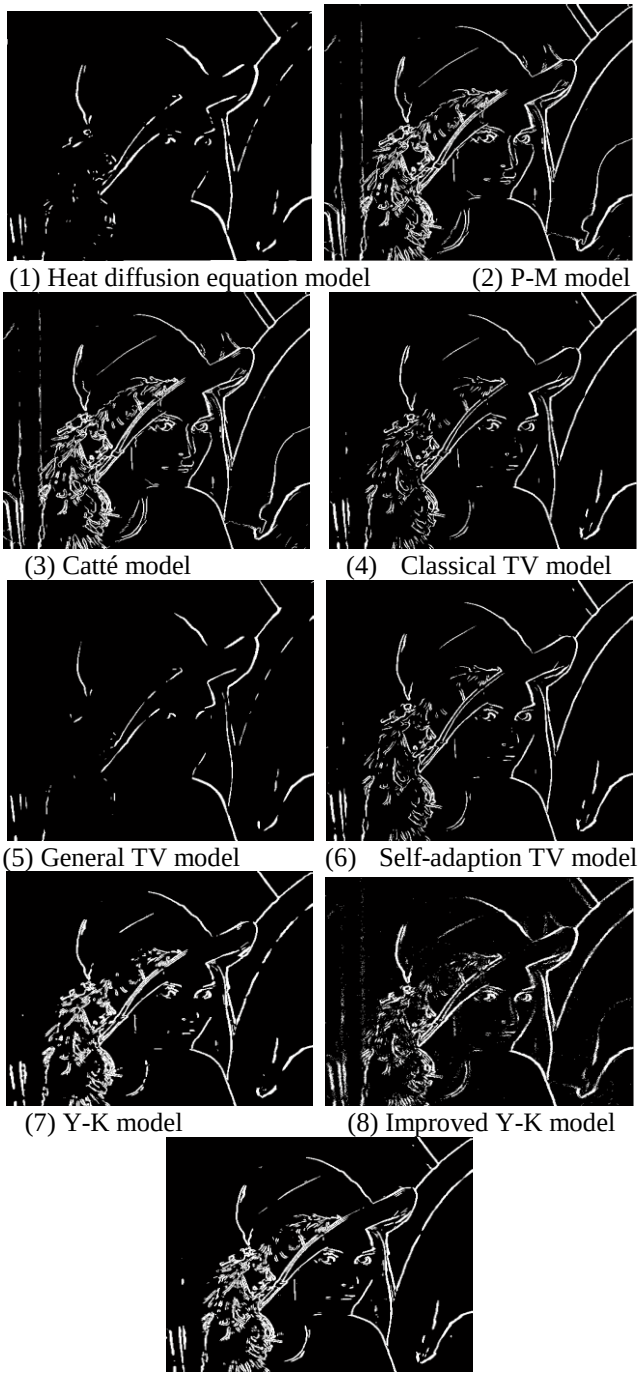

(1) Heat diffusion equation model (2) P-M model
(3) Catté model (4) Classical TV model
(5) General TV model (6) Self-adaption TV model
(7) Y-K model (8) Improved Y-K model
(9) Model stated in this paper

Fig. 1 Comparison of Lena Image Edge Detection Results of 9 Types of Models

As is shown in the comparison of detection results, in the condition without noise interference, the edge detection effects obtained through the heat equation diffusion model and General TV(P=1.5) model are most unsatisfactory in the subjective evaluation method system; there are only a few of discontinuous edge pixel points and there is a serious lack of edge pixel points in the hair texture part of Lena. The P-M model and the Catté model are basically the same. The P-M method can be theoretically proven to be "morbid"; i.e. any subtle changes in the input will lead to complete changes in output. However, as this experiment is free of noise interference and the Lena images inputted in the two groups are totally the same, the edge extraction effects obtained from the detection of the two models should be the same. The classical TV model and the self-adaption model are generally the same and one cannot tell which one is better through

observation with naked eyes; as for the Y-K model and the improved Y-K model, the former one is obviously superior to the latter one in the number of edge pixel points, hair texture part and edge continuity etc. As for the new model put forward in this paper, even though there is an edge loss in on the left side of image, the capturing of weak edge, preservation of hair texture part and elimination of false edge are improved.

In order to verify the conclusion made through the above-mentioned subjective evaluation method, the objective evaluation index $EIdx$ of numerical edge detection was used for verification. Besides, the evaluation index includes three benchmark evaluation parameters, which are respectively the edge detection image reconstruction similarity $SSIM$, edge reliability $BIdx$ and edge continuity $CIdx$. The evaluation results are shown in Table 1 and Fig. 2.

It can be seen that the comparison of numerical edge detection evaluation indexes verified the conclusion made through the above-mentioned subjective evaluation method:

(1) The edge detection evaluation indexes of heat equation diffusion model and General TV (P=1.5) model are the smallest.

(2) P-M model and Catté model are completely the same in the edge detection image reconstruction similarity index, edge reliability index and edge continuity index; i.e. they are totally the same.

(3) As for the classical TV model and self-adaption TV model, if one cannot tell which detection result is better through observation with naked eyes, the evaluation index can correctly show that the classical TV model is superior to the self-adaption TV model.

(4) Through the comparison of edge detection evaluation indexes of the classical Y-K model and the improved Y-K model, the latter one is far superior to the former one.

(5) The edge detection evaluation index $EIdx$ of the new model put forward in this paper is the biggest among all models.

Table 1 Edge Detection Evaluation Indexes of Lena Image of 9 Models

Image		Image with noise			
Evaluation index		SSIM	BIdx	CIdx	EIdx
Methods	Heat equation diffusion	0.8245	0.1917	0.9171	0.5701
	P-M	0.8998	0.1597	0.9723	0.7187
	Catte	0.8998	0.1597	0.9723	0.7187
	Classical TV	0.8345	0.2165	0.9718	0.7247
	General TV (P=1.5)	0.5795	0.2806	0.8426	0.5704
	Self-adaption TV	0.8348	0.2163	0.9378	0.6992
	Classical Y-K	0.8163	0.1777	0.9485	0.6801
	Improved Y-K model	0.9035	0.1552	0.9852	0.7243
	Model stated in this paper	0.8491	0.1657	0.9558	0.733

$*SSIM$ - edge detection image reconstruction similarity; $BIdx$ - edge reliability; $CIdx$ - edge continuity; objective evaluation index of edge detection $EIdx$

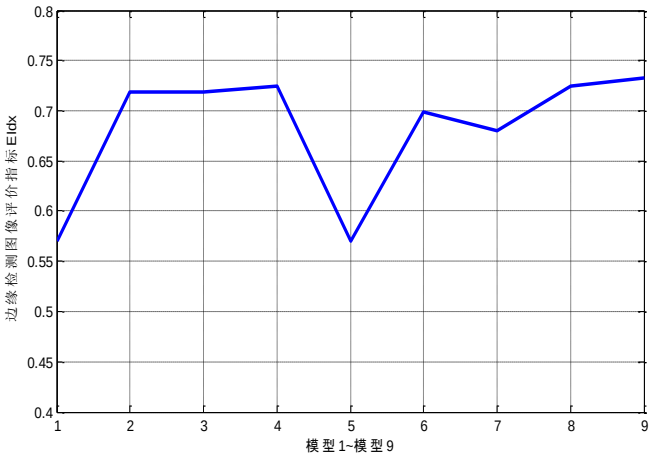

Fig. 2 Curve Graphs for Edge Detection Evaluation Indexes of Lena Image of 9 Models

B. Experiment II

For the purpose of crosswise comparison, we used a teaching building as the test image (as shown in Fig. 3) without Gaussian white noise; i.e. we used the original pollution-free main teaching building test image to verify the validity of new model. The test results of the 9 models are shown in Fig. 4.

It is found through the comparison of detection results that the edge detection effects obtained from the heat equation diffusion model and the General TV (P=1.5) model are most unsatisfactory and the edge loss is most severe in the subjective evaluation method system under the condition without noise interference. The P-M model and the Catté model are basically the same and one cannot tell whose effect is better with naked eyes. The classical TV model and the self-adaption model are generally the same; as for the classical Y-K model and the improved Y-K model, the former one is obviously superior to the latter one in the number of edge pixel points and texture preservation function. The new model put forward in this paper is superior to the other eight ones in the number of edge pixel points, texture edge preservation function and edge continuity.

In order to verify the result obtained through the above-mentioned subjective evaluation method, we continued to use the objective evaluation index of numerical edge detection for verification, as shown in Table 2 and Fig. 5:

It can be found that the comparison of numerical edge detection image evaluation indexes mentioned above can still lead to the conclusion made through the above-mentioned subjective evaluation method.

(1) The edge detection evaluation indexes of heat equation diffusion model and General TV(P=1.5) are still the worst among all models.

(2) The P-M model and Catté model are completely the same in the edge detection image reconstruction similarity index, edge reliability index and edge continuity index; namely, they are totally the same. This re-verifies that the P-M model and Catte model have the same edge extraction effect without noise interference.

(3) As for the classical TV model and self-adaption TV model, if one cannot tell whose detection effect is better with naked eyes, the evaluation index can correctly show that the self-adaption model is slightly superior to the classical TV model.

(4) Through the comparison of edge detection evaluation indexes of classical Y-K model and improved Y-K model, the latter one is slightly inferior to the former one.

(5) The new model put forward in this paper has good performance in the edge detection image reconstruction similarity index $SSIM$, edge reliability index $BIdx$ and edge continuity index $CIdx$. Its edge detection image evaluation index $EIdx$ is 1% to 4% higher than that of all other models.

Fig. 3 Teaching Building Test Chart for Crosswise Comparison

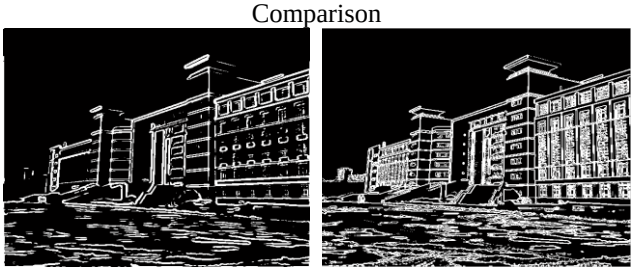

(1) Heat diffusion equation model (2) P-M model

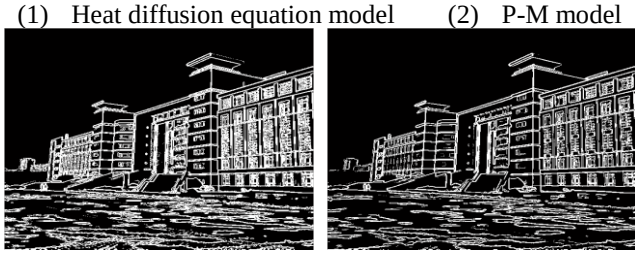

(3) Catté model (4) Classical TV model

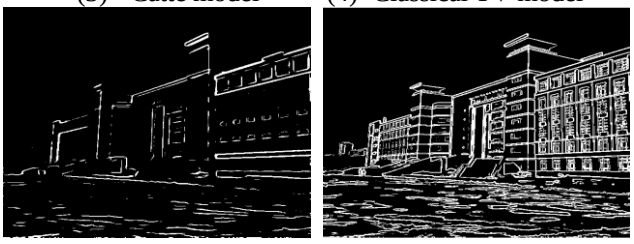

(5) General TV model (6) Self-adaption TV model

(7) Y-K model (8) Improved Y-K model

(9) Model stated in this paper

Fig. 4 Comparison of Teaching Building Image Edge Detection Results of 9 Models

Table 2 Evaluation Indexes for Teaching Building Image Edge Detection of 9 Models

Image		Image with noise			
Evaluation index		SSIM	BIdx	CIdx	EIdx
Methods	Heat equation diffusion	0.8656	0.2701	0.9755	0.691
	P-M	0.8837	0.2602	0.9951	0.7238
	Catte	0.7238	0.2602	0.9951	0.7238
	Classical TV	0.8746	0.314	0.9933	0.7437
	General TV (P=1.5)	0.6698	0.3929	0.9622	0.6739
	Self-adaption TV	0.8747	0.3149	0.9932	0.7439
	Classical Y-K	0.8826	0.2452	0.9952	0.7158
	Improved Y-K	0.8724	0.2266	0.9931	0.7149
	Model in this paper	0.8852	0.2518	0.9949	0.7544

* $SSIM$ - edge detection image reconstruction similarity; $BIdx$ - edge reliability; $CIdx$ - edge continuity; objective evaluation index of edge detection $EIdx$

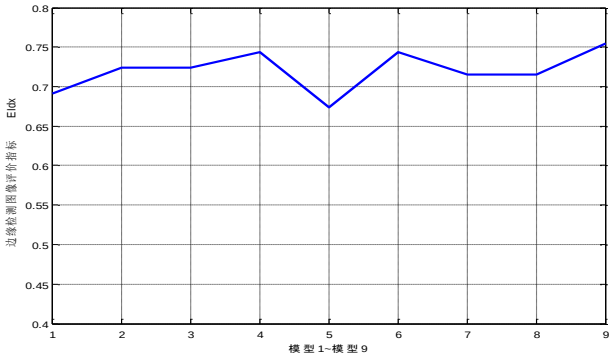

Fig. 5 Curve Graph for Evaluation Indexes of Building Image Edge Detection of 9 Models

V. CONCLUSION

After the application of the traditional second-order partial differential equation and the four-order partial differential equation in image edge detection was analyzed, a conclusion was made on the advantages and disadvantages of the second-order and high-order partial differential equations; then, a new edge extraction mode based on the second-order and high-order partial differential equations was obtained by preserving their advantages and eliminating their disadvantages, namely, by integrating the advantages of second-order and high-order partial differential equations. The model can not only effectively overcome the common problem of "staircase effect" of second-order partial differential equation but also effectively restrain the advantages, such as "speckle effect" and inaccurate edge positioning, of four-order partial differential equation. The Euler-Lagrange equation for the new model was solved to lead out the gradient descent flow, and the numerical discretization method was given for the purpose of the follow-up numerical calculation. In order to make crosswise comparisons, two experiments were conducted in the experimental process of this paper. Experiment I was to conduct the edge extractions for the traditional second-order partial differential equation, four-order partial differential equation and new model respectively for the Lena image without noise interference. Experiment II was to conduct the edge extractions for the traditional second-order partial differential equation, four-order partial differential equation and new model respectively for the building image. Finally,

the subjective and objective evaluation systems of edge evaluation were used to evaluate the test result. The evaluation result shows that the new model has good edge detection ability. In the future, it is required to further study the existence and uniqueness of solutions of second-order and four-order partial differential equation models as well as the optimal stopping time of edge extraction etc.

REFERENCES

[1]Chen, Q., Montesinos, P., Sun,Q.S.et al. Adaptive total variation denoising based on difference curvature[J].Image and Vision Computing, 2010, 28(3): 298-306.

[2]HAN Shou-Dong, ZHAO Yong, TAO Wen-Bing,etc. Gaussian Super-pixel Based Fast Image Segmentation Using Graph Cuts [J]. ACTA AUTOMATICA SINICA. 2011(01):33-37.

[3]Cai Zhanchuan, Yao Feifei,Tang Zesheng. Digital Image Inpainting with Krigin Method[J].Journal of Computer-Aided Design &Computer Graphic,2013(09):56-59.

[4]Zhang Zhi-lanbao,Zhang Jian-guo. Research on Recognition Methods and Function Based on New Pattern Recognition [J]. Science and technology innovation and productivity, 2011(06):25-29.

[5]Witkin A..Scale space filtering[C]. In Proceeding of 8th International Joint Conference of Artificial Intelligence,Vol.2:1019-1022.

[6]Perona, P.,Malik, J.Scale-space and edge detection using anisotropic diffusion[J].Patternn Analysis and Machine Intelligence,IEEE Transactions on,1990,12(7):629-639.

[7]Catté, F.,Lions, P.-L.,Morel, J.-M. et al.Image selective smoothing and edge detection by nonlinear diffusion[J].SIAM Journal on Numerical Analysis ,1992,29(1):182-193.

[8]Rudin,L.I.,Osher,S.,Fatemi,E.Nonlinear total variation based noise removal algorithms[D].Nonlinear Phenomena, 1992, 60(1): 259-268.

[9]Song, B.Topics in variational PDE image segmentation in painting and denoising[D],University of California Los Angeles, 2003.

[10] ZHANG Hong-ying,PENG Qi-cong. Adaptive image denoising model based on total variation [J]. Opto-Electronic Engineering ,2006(03):50-53.

[11] You, Y.-L.,Kaveh, M.Fourth-order partial differential equations for noise removal[J].ImageProcessing,IEEE Transactions on, 2000, 9(10): 1723-1730.

[12] ZHOU Qian, ZHAO Fang-ling, ZHAO Feng-qun. An Improved Coef ficient of the You-Kaveh' s Image Denoising Model [J]. COMPUTER ENGINEERING & SCIENCE.2010,3(02):37-40.

[13] Jiang Gang-yi,Huang Da-jiang. Overview on Image Quality Assessment Methods [J]. Journal of Electronics & Information Technology，2010,32(1):220-226.

[14] LIN Hui,ZHAO Chang-sheng,SHU Ning. Edge detection based on Canny operator and evaluation[J].Journal of Heilongjiang Institute of Technology,2003, 17(2):3-6.

[15] Chen, Q., Montesinos, P., Sun,Q.S.et al. Adaptive total variation denoising based on difference curvature[J].Image and Vision Computing, 2010, 28(3): 298-306.

Author Name : YU Bo-wen

Publications : Communication Module of FC-AE-1553 Interface
Improved Apriori Algorithm Based on Matrix Reduction